Reversible faceting of the copper (110) surface: X-ray Fresnel reflectivity

B. M. Ocko
Physics Department, Brookhaven National Laboratory, Upton, New York 11973

S. G. J. Mochrie*
AT&T Bell Laboratories, Murray Hill, New Jersey 07974
(Received 2 March 1988)

We have investigated the thermodynamic stability of copper surfaces with small misalignments from the [110] direction using x-ray Fresnel reflectivity. We find that the misaligned orientation is stable only at high temperatures. At low temperatures the surface breaks up into a hill-and-valley structure of predominantly (110) facets. This process is reversible. Exposure of the surface to O_2 increases the stability of the (110) facets, counter to simple theoretical ideas.

I. INTRODUCTION

A crystal can be cut in an arbitrary direction; but if that orientation does not appear on the equilibrium form, then a *hill-and-valley* structure[1,2] consisting of macroscope regions of allowed orientation will inevitably replace it. For example, in a recent low-energy electron diffraction (LEED) experiment on clean Si surfaces, Phaneuf and Williams[3] showed that a range of orientations near the [111] direction was unstable at low temperatures. Rather than conform to the imposed misorientation, the Si surfaces form (111) facets where the surface is aligned with the crystallographic planes, together with regions of high step density. This faceting[3] can be understood in terms of a lower surface free energy of the (111) facet as a result of its (7×7) reconstruction[4] relative to that of the stepped regions which remain unreconstructed. The detailed temperature dependence of the step separation is determined by the repulsive interaction between the steps.

X-ray Fresnel reflectivity has proven to be a powerful probe of the microscopic structure of liquid[5] and liquid-crystal surfaces[6] and one may anticipate that such measurements will also provide interesting information about solid surfaces. In this paper we report measurements on the *equilibrium* behavior of copper surfaces with a small misalignment away from the [110] direction. Copper surfaces have been studied both experimentally and theoretically and it seems that a detailed understanding of their thermodynamic behavior from microscopic interactions should be possible. In addition, a previous x-ray study,[7] using one of our samples, showed that the copper (110) facet was unstable with respect to a rough phase for $T>870$ K. However, the importance of the misorientation only emerged during the present work. We show that important information can be extracted from Fresnel reflectivity measurements, even from a typically imperfect metal crystal. Remarkably, at low temperatures the Fresnel reflectivity corresponds to a direction which is accurately aligned along the Bragg plane normal. At high temperatures, however, the reflectivity reverts to the mean surface-normal direction.

II. X-RAY REFLECTIVITY

The x-ray scattering cross section $(d\sigma/d\Omega)$ from a predominantly planar interface may be calculated within the distorted-wave approximation:[8,9]

$$d\sigma/d\Omega=r_0^2\,|\,T(\theta_1)T(\theta_2)\,|^2 VS(\mathbf{Q})\ , \tag{1}$$

where r_0^2 is the Thomson radius, V is the scattering volume, $S(\mathbf{Q})$ is the Fourier transform of the (electronic) density-density correlation function, $90-\theta_1$ and $90-\theta_2$ are the angle the incident and scattered x ray, respectively, make with the surface normal, and $T(\theta_1)$ and $T(\theta_2)$ are the corresponding Fresnel coefficients of classical optics. The explicit form of $T(\theta)$ is

$$T(\theta)=\frac{2\sin\theta}{\sin\theta+(\cos^2\theta_c-\cos^2\theta)^{1/2}}\ . \tag{2}$$

For a perfectly flat surface between a material of uniform electronic density (ρ_0) and the vacuum, Eq. (1) yields

$$d\sigma/d\Omega=\rho_0^2 r_0^2\,|\,T(\theta_1)T(\theta_2)\,|^2 4\pi^2 A\,\delta(Q_x)\delta(Q_y)/Q_z^2\ , \tag{3}$$

where A is the illuminated area, Q_z is the momentum transfer normal to the surface, and Q_x and Q_y are the parallel components.

When the spectrometer is set to the specular condition, i.e., $\theta_1=\theta_2=\theta$, as shown in Fig. 1, the measured reflectivity is given by the differential cross section integrated over the range of angles accepted by the detector. We must also normalize to the incident beam area and take into account that the total number of counts within the resolution volume must be given by the number of incident x rays. The latter determines the weighting of the resolution volume to be $(\Delta\theta_1)^{-1}$, so that

 ©1988 The American Physical Society

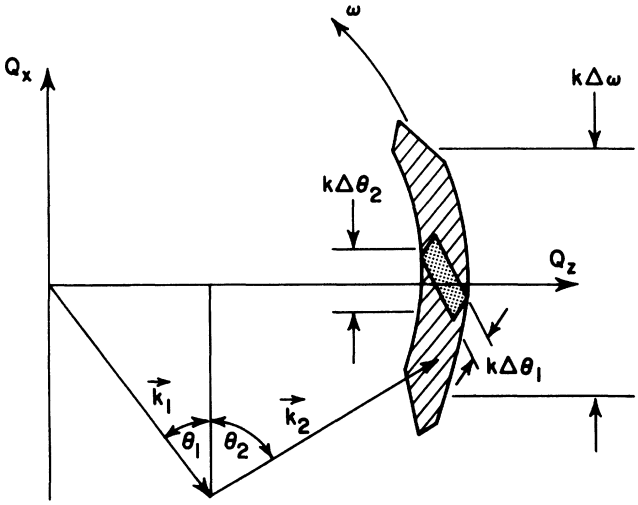

FIG. 1. The x-ray resolution volume projected onto the scattering plane. The shaded area is the resolution trapezoid defined by the spread of the incoming beam ($\Delta\theta_1$) and the acceptance of the detector slit ($\Delta\theta_2$). The resolution area swept out by scanning ω over a range $\Delta\omega$ is given by the hatched arc.

$$R A_0 = \frac{1}{\Delta\theta_1}\int (d\sigma/d\Omega)d\Omega$$

$$= 4\pi^2 A L \Delta Q_z \,|\, T(\theta) \,|^4 \frac{\rho_0^2 r_0^2}{Q_z^2} \Big/ (\Delta\theta_1) \,, \quad (4)$$

where $L = [k^3 \sin(2\theta)]^{-1}$ is the usual Lorentz factor, relating a volume in reciprocal space to one in angle space, and $\Delta Q_z = 2k\Delta\theta_1 \cos\theta$, as is clear by inspection of Fig. 1. The illuminated area, in the limit that the incident beam does not spill over the sample, is $A = A_0/\sin\theta$, where A_0 is the incident beam area. Then, Eq. (4) becomes

$$R = 16\pi^2 r_0^2 \rho_0^2 \,|\, T(\theta) \,|^4 / Q_z^4 \,. \quad (5)$$

This is the usual expression for Fresnel reflectivity.

As noted above, particular surface orientations do not necessarily appear in equilibrium. Instead the surface can rearrange itself on long length scales (limited by kinetics) into Herring's hill-and-valley structure.[1] The signature of such behavior is particularly dramatic. The x-ray Fresnel reflectivity will no longer be specular with respect to the macroscopic cut of the crystal—the *optical* surface normal—instead, it will occur in a direction determined by the microscopic surfaces which are now exposed. For a hill-and-valley surface, Eq. (3) must be modified since the surface is no longer perfectly flat. In addition, Eq. (5) must be modified to account for the correct number of surface atoms.

If the microscopic surface height $[u(\mathbf{r})]$ varies across the crystal, then the phase difference associated with the different heights modifies the form of $S(\mathbf{Q})$.[5,10–12]

$$VS(\mathbf{Q}) = A\frac{\rho_0^2}{Q_z^2}\int d^2r\, e^{i\mathbf{q}_t\cdot\mathbf{r}} e^{-Q_z^2\langle[u(\mathbf{r})-u(0)]^2\rangle/2} \,, \quad (6)$$

where $\mathbf{q}_t = (Q_x, Q_y, 0)$ and $\mathbf{r} = (x, y, 0)$, and we have assumed that $u(\mathbf{r})$ is a Gaussian random variable. Thus, the behavior of the surface shows up directly in the cross section via the height-height correlation function, $C(\mathbf{r}) = \langle [u(\mathbf{r}) - u(\mathbf{0})]^2 \rangle$. An important physical quantity describing a liquid surface is its surface tension (α).[13] The excess free energy contained within capillary modes on a liquid surface is given by

$$F = \frac{\alpha}{2}\int d^2r (\nabla u)^2 \,. \quad (7)$$

From the equipartition theorem,

$$C(\mathbf{r}) = \frac{k_B T}{2\pi\alpha}\ln(r/a) \,, \quad (8)$$

where a is a microscopic length. For a crystal surface, α depends on the orientation (ϕ) of the surface with respect to the crystalline axes.[1] In this case capillary fluctuations are controlled by the surface stiffness, $\gamma = \alpha + d^2\alpha/d\phi^2$.[14,15] Facets on the equilibrium crystal shape (ECS) (Ref. 2) correspond to cusps in $\alpha(\phi)$, so that $d^2\alpha/d\phi^2$; and thus γ is infinite for those orientations. Equation (8) applies equally to crystal surfaces if the surface tension (α) is replaced by the surface stiffness (γ). By combining Eqs. (6) and (8), we find[16]

$$VS(\mathbf{Q}) = A\frac{\rho_0^2 a^2}{Q_z^2}\left[\frac{\Gamma(1-\eta/2)}{\Gamma(\eta/2)}(q_t a)^{-2+\eta} - \frac{1}{1-\eta/2}\right] \,, \quad (9)$$

where $\eta = k_B T Q_z^2/2\pi\gamma$. Instead of the scattering being confined to discrete values of q_t, as for the flat surface [Eq. (3)], now it is diffuse in a manner determined by the surface stiffness. Equation (9) is inappropriate for orientations that correspond to facets on the ECS. For those directions the surface stiffness is infinite and Eq. (3) represents the expected form of the reflectivity, albeit with an additional Q_z-dependent Debye-Waller-like factor. Both Eqs. (3) and (9) are only valid when the crystalline lattice structure can be neglected; this is appropriate at small angles, far from Bragg peaks. Extensions to include the lattice structure are presented elsewhere.[17] Because of the fine reciprocal-space resolution which is available with present-day x-ray sources, it should be possible to distinguish between the scattering from an atomically-smooth surface [Eq. (3)] and a rough surface [Eq. (9)]. At any finite spectrometer resolution Eq. (9) leads to an "effective" specular reflectivity which can be interpreted in terms of a root-mean-square (rms) roughness.[5]

III. PREVIOUS RESULTS

Observation of small copper crystals immediately below their melting point ($T_m = 1356$ K) demonstrates that the (110) facet is absent from the ECS at this temperature.[18] This requires that either (a) the (110) facet has a roughening transition at a temperature (T_R) below T_m or (b) the (110) is not a stable facet at any temperature. The latter possibility would occur if the surface free energy of, say, the (111) facet were so much lower than that of the

(110) surface that it would be energetically favorable for the surface to increase its area to form (111) facets, rather than a flat (110) surface.

For Cu(110), Mochrie[7] has shown that the (110) surface is well-defined over length scales of several thousand angstroms, in striking contrast to the much smaller length scales measured for the Ag(110) (Ref. 19) surface and Cu and Ni(100) vicinal surfaces.[20–22] Together with Ref. 18, Ref. 7 provided the first direct demonstration that the (110) facet of Cu is a stable equilibrium facet at low temperatures and becomes unstable at higher temperatures.

IV. EXPERIMENT

The experiments reported here were conducted at Brookhaven using a 12-kW rotating-anode x-ray source. A Ge monochromator was set to accept Cu $K\alpha$ radiation ($\lambda=2\pi/k=1.54$ Å). The sample was contained within a vacuum chamber that mounts directly onto a standard four-circle diffractometer.[7] The temperature was varied by adjusting the current through a tungsten filament which heated the back of the sample radiatively. The base pressure of the chamber was 1×10^{-9} Torr with the sample at room temperature. When the sample was held at $T=970$ K the pressure reached 9×10^{-9} Torr. Surface cleaning was accomplished by Ar^+-ion bombardment (1 μA and 500 V). Since standard polishing procedures cause a slight bowing of the crystal surface, especially near the edges, care was taken to illuminate as small a region as possible near the center.

The x-ray spot size was controlled by a defining slit close to the sample. Typically a beam 0.1 mm$\times$2 mm in area was used, which illuminated an area 4.5 mm$\times$2 mm at an incidence angle of 1.25°. Approximately $4\times10^{+5}$ photons per second were incident on the sample. The finite x-ray source size on the anode collimated the incoming beam in the scattering plane to $\Delta\theta_1=0.001°$ FWHM for the narrowest slits. This in turn produced a minimum beam width at the sample position of 0.1 mm. The spectrometer resolution (see trapezoid in Fig. 1) was determined by the divergence of the incoming x-ray beam and the acceptance of the scattered x rays by the detector slit. In the scattering plane, the outgoing divergence ($\Delta\theta_2=0.05°$ FWHM) was fixed by the detector slit width. Out of the scattering plane, the resolution was $\Delta\chi_2=1.0°$ FWHM.

For perfectly flat and crystallographically aligned samples, the acceptance angle of the detector need only be as large as $\Delta\theta_1$ to collect all of the reflected intensity. However, for nonideal samples the scattering is distributed over a range of exit angles determined by the sample mosaic. To properly integrate over this mosaic the transverse resolution must be broader than the features of the mosaic. The in-plane resolution can be coarsened by increasing the detector width (i.e., $\Delta\theta_2$), however there is a concomitant increase in the longitudinal resolution. For the integrated reflectivity measurements we have chosen to integrate over a range of $\omega=\theta-(2\theta)/2$ at constant 2θ, by rocking the sample as shown by the arc in Fig. 1. Under these conditions, the reflectivity is given by

$$R=\frac{\int d\theta\, I_s(\theta)}{\frac{1}{2}\int d(2\theta) I_0(2\theta)}\,, \tag{10}$$

where $I_s(\theta)$ is the scattered intensity after background subtraction and $I_0(2\theta)$ is the direct beam intensity. This configuration allows us to simultaneously measure the transverse scans and the absolute reflectivity with reasonable Q_z resolution.

V. RESULTS

We have performed measurements on two different samples. The first sample (sample 1), which proved to have a misalignment of 0.8° away from the [110] direction, was the same as used in Ref. 7. The second sample[23] (sample 2) had a misorientation of only 0.2°.

First, we will present our results obtained on sample 1. Figure 2 shows scans transverse to the reflectivity at several different wave vectors (Q_z) and two temperatures as a function of $\omega=\theta-2\theta/2$. By definition, at $\omega=0$ the scattering vector is aligned normal to the (110) crystalline planes. At high temperatures ($T=900$ K), as shown in Fig. 2(a), the reflectivity corresponds to a direct that is displaced towards larger ω by 0.8°. Thus, surface must be stepped over the coherence area of the spectrometer since the scattering is not centered around $\omega=0$. A Lorentzian line shape with $\Delta\omega$ fixed at 0.20° half width at half maximum (HWHM) provides a reasonable description of the data at all Q_z [solid lines in Fig. 2(a)]. Unfortunately, the

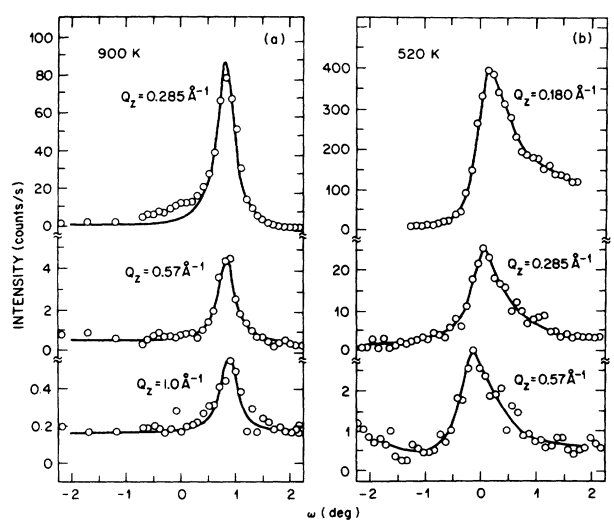

FIG. 2. X-ray scattering intensity at several wave vectors vs the sample orientation ($\omega=\theta-2\theta/2$ for sample 1). (a) At $T=900$ K the Fresnel reflectivity occurs along the direction of the misalignment (i.e., th mean surface normal). The line shapes are nearly symmetric, except at small wave vectors where there is additional scattering at $\omega\simeq0$. The solid lines are Lorentzian line shapes with $\Delta\omega=0.2°$ HWHM as described in the text. (b) At $T=520$ K the Fresnel reflectivity occurs close to the [220] direction ($\omega=0$). The line shapes exhibit a pronounced asymmetry with additional scattering towards the misorientation direction. The solid lines are guides to the eye.

width of the profiles is rather large by high resolution x-ray scattering standards. Furthermore, at the smallest wave vectors there is additional scattering near $\omega=0$.

In a reflectivity experiment, the transverse linewidth (ΔQ_z) depends on (i) the microscopic correlation length of the surface (L), (ii) the macroscopic distribution of surface normals across the sample ($\Delta\omega_n$), and (iii) the spectrometer resolution. For perfectly correlated and perfectly flat samples, $\Delta Q_x = Q_z \Delta\theta_2$. For our experimental parameters $(Q_z\Delta\theta_2)^{-1}$ ranges from 10 000 to 2000 Å as Q_z varies between 0.20 and 1.0 Å^{-1}. For imperfect samples, we have $\Delta\omega_n > \Delta\theta_2$ and/or $(LQ_z)^{-1} > \Delta\theta_2$, the transverse width depends both on L and ω_n. If we attribute all of the observed transverse width ($Q_z\Delta\omega$) to a finite correlation length then $L=(Q_z\Delta\omega)^{-1} \sim 1000$ Å^{-1} (as calculated at $Q_z=0.2$ Å^{-1}). Since the transverse profile does not evolve with Q_z the dominant effect on the line shape must be the distribution of surface normals, L *must be greater than* 1000 Å. Since $\Delta\omega$ varies by $\pm 15\%$ (as Q_z increases by a factor of 5), the data certainly does not support the Q_z dependence expected for finite-size regions: $\Delta\omega=(LQ_z)^{-1}$. Furthermore, the observed Q_z independence of $\Delta\omega$ cannot be explained within the context of simple models of intrinsic disorder ($\Delta Q_x \propto Q_z^2$).

Suppose that the steps are of height h, then the change in phase going across a step is $Q_z h$. For a model with randomly distributed steps, the x-ray reflectivity will lie along the optical normal at small Q_z if $Q_z h < 1$ rad, otherwise each microterrace will contribute independently. At $Q_z=1$ Å^{-1} we therefore require that $h \leq 1$ Å. The only possible step that can satisfy this condition is monatomic, with $h=d=1.28$ Å. In this case the mean step separation is 90 Å$=1.28$ Å/tan(0.8°).

Figure 3 displays the integrated intensity of each ω scan as a function of Q_z at $T=900$ K. The solid line is the calculated Fresnel reflectivity for a perfectly flat interface [Eq. (5)]. As noted above, absolute measurements were limited to $Q_z > 0.18$ Å^{-1}. The close agreement between the calculation and the data implies that the surface is microscopically very flat. Indeed, the deviation can be accounted for by a root-mean-square (rms) roughness of the order of 1 Å. However, because of the $\Delta\omega$ width at $Q_z \geq 1$ Å^{-1}, we can only say that regions of size of order 1000 Å have this rms roughness; we cannot determine whether the power-law from [Eq. (9)] is applicable. For liquid copper, such a value for the rms roughness is expected on the basis of capillary theory [Eq. (8)], using the surface tension of liquid copper for γ (Refs. 5 and 7).

Figure 2 also shows ω scans at $T=520$ K. Although the profiles are asymmetric, the integrated intensities are within 30% of the values obtained at 900 K over the range $0.3 < Q_z < 0.8$ Å^{-1}. Therefore, the effective roughness at both temperatures is comparable. The profiles (Fig. 2) exhibit additional scattering towards the misaligned direction. Even with the asymmetry, the reflectivity corresponds to a direction which, in spite of the misorientation, is accurately ($\pm 0.1°$) aligned along the normal to the [110] crystalline direction. It is clear that the surface undergoes a transition from a region of

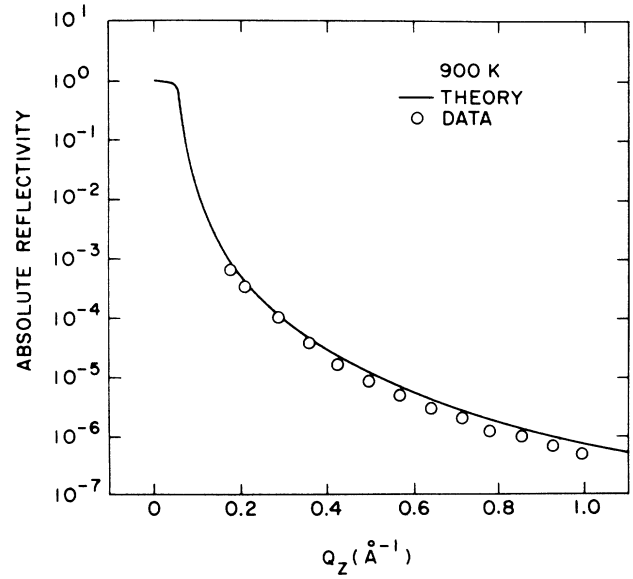

FIG. 3. Absolute reflectivity at $T=900$ K. The open circles are the result of integrating ω scans (see Fig. 2) which are normalized to the incident flux [Eq. (10)]. The solid line is the Fresnel law of optics for an ideal copper interface. Because of the close agreement between the calculation and the data, microscopically the surface is very flat. The deviation may be accounted for by a root-mean-square roughness of less than 1 Å.

stability of the (110) facet at low temperatures to one at elevated temperatures in which the surface behaves like a liquid surface minimizing its surface area.

In order that the surface at low temperatures be composed of large (110) facets of order several thousand angstroms and maintain the overall as-cut orientation on millimeter length scales, there must be other regions which make an angle larger than the mean with the [110] direction. Such orientations could correspond to other high-symmetry directions—(111) or (100) facets—or they could simply be regions of high step density. Unfortunately, if these latter regions are small, their scattering will be weak and diffuse. Our scans did not extend beyond $\omega=2°$, to the angles where we would expect such scattering to appear. If there are regions of high step density, it implies that the steps experience a mutual attraction. Such behavior does not arise in surface models with only nearest-neighbor interactions. It does, however, emerge from a mean-field calculation including repulsive next-nearest-neighbor interactions. But whether this behavior survives the introduction of fluctuations is in question.[24] In the case of the misoriented Si(111),[3] there is an effective attraction between steps because the (111) facets reconstruct whereas the stepped regions do not. Therefore, to take advantage of the reconstruction the steps are squeezed closer together. Such an argument cannot be made here, since the clean Cu(110) surface is not known to reconstruct. However, it is well known that small amounts of oxygen produce a 1×2 reconstruction on the Cu(110) surface.[25,26] The effect of oxygen on sample 2 will be discussed below.

Sample 2 had a smaller misalignment (0.2°) and a smaller $\Delta\omega$ width, at least at low temperatures. Its behavior, however, is qualitatively similar to that of sample 1. In Fig. 4, we show the profiles observed both when the misalignment lies within the scattering plane ($\phi=0°$) and when the misorientation is normal to the scattering plane ($\phi=90°$). All of the out-of-plane scattering is accepted by the detector slits. These data correspond to $Q_z=0.28$ Å^{-1} and in the rough phase at this small wave vector the exponent η will only have achieved a rather small value, say $\eta=0.05$ using the parameters appropriate for liquid copper. Previous studies of other systems with power-law line shapes have shown that such small values of η are difficult to distinguish from delta-function line shapes. Thus, intrinsic capillary fluctuations should produce little change in the line shape at $Q_z=0.28$ Å^{-1} in going from the faceted phase to the rough phase. This expectation notwithstanding, it is evident that the profile at $\phi=90°$ in the high-temperature, rough phase is different from that in the low-temperature faceted phase—the tails of the profile are substantially enhanced at high temperatures.

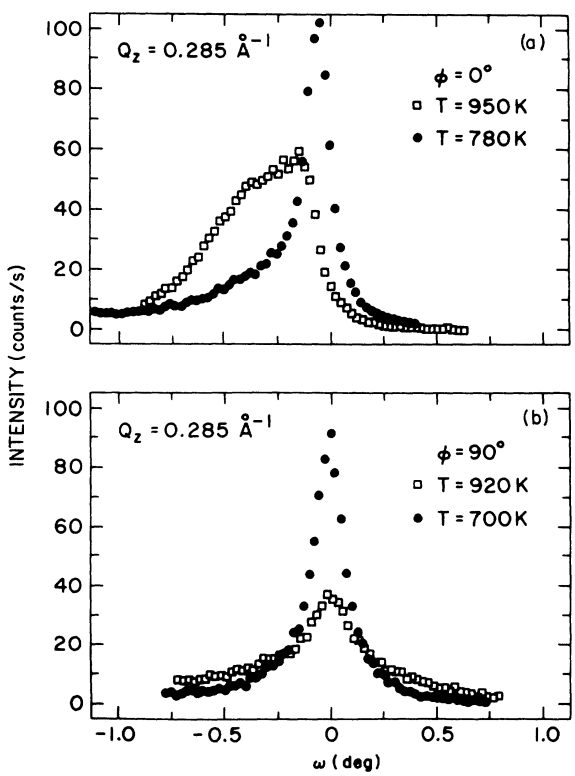

FIG. 4. X-ray scattering intensity at several wave vectors vs the sample orientation ($\omega=\theta-2\theta/2$ for sample 2). The ϕ axis is parallel to the [110] direction. (a) $\phi=0$ corresponds to the misorientation lying within the scattering plane. There is a dramatic change in the profile shapes and positions for the data above and below the roughening transitions. (b) $\phi=90$ corresponds to the misorientation being normal to the scattering plane. There is no change in the peak position and a moderate change in the profile shape for the data above and below the roughening transition.

At elevated temperatures, the surface orientation is determined by the local misorientation of the surface away from the [110] direction. If there is a distribution of misalignments across the sample, that will result in a distribution of the direction of the scattering. The extent of the broadening does not depend on microscopic details, but on the quality of the macroscopic surface finish. On the other hand, at low temperatures the observed reflectivity is due to (110) facets, whose orientation is aligned along the crystalline axis with a profile determined by the bulk crystalline mosaic. Therefore, the increased scattering in the wings of the high-temperature scattering line shape is produced by the distribution of the optical surface normal which is broader than the sample mosaic.

Figure 4 also shows profiles transverse to the [110] direction ($\omega=0°$) when the misalignment is within the scattering plane ($\phi=0°$). At low temperatures the data consist of a sharp peak at $\omega=0$ with a FWHM of 0.2°—the same as the bulk mosaic—together with a broad feature at angles smaller than $\omega=0$. This is the direction of the imposed misorientation. These data suggest that perhaps the regions complementary to the (110) facets are regions of high step density corresponding to this broad, low-angle feature. Again, our data do not extend to sufficiently small angles to allow us to make this identification unambiguously. At the highest temperature that we were able to achieve ($T=950$ K), the peak of the profile has shifted towards the smaller angles. However, it has not acquired the symmetrical shape that was observed for sample 1 at $T=900$ K. We have attempted to describe these profiles using models that incorporate no long-ranged correlations between steps.[27] However such models do not provide a satisfactory description of the Q_z dependence of the data.

Copper is a reactive material and we were concerned to investigate the role that surface contamination might play and ensure that in fact it did not effect our results. To this end we conducted a number of experiments. The most reliable technique for determining what is on a surface is Auger electron spectroscopy. However, our chamber was not equipped to do this. Therefore, we had to be satisfied with cleaning our sample surface frequently enough that the measurements obtained between cleaning cycles are always reproducible. In addition, assuming that O_2 was the most likely contaminant, we crudely investigated the effect of dosing the sample with O_2, when it was held at around $T=920$ K—which is above the faceting transition temperature. Surprisingly, this caused the microscopically stepped surface to develop (110) facets, as would have occurred if the clean surface had been lowered in temperature. The change in the equilibrium surface stability may be related to the adsorption of oxygen. At lower temperatures it is known that oxygen induces a 2×1 reconstruction.[25,26] Faceting was also observed if the sample was left without sputtering for a long time. The waiting time typically varied from 12 to 24 h, presumably depending on the partial pressure of O_2 in the chamber—this was always below the sensitivity of our mass spectrometer. Figure 5 shows the transition as monitored by the change in the width of the profile (sam-

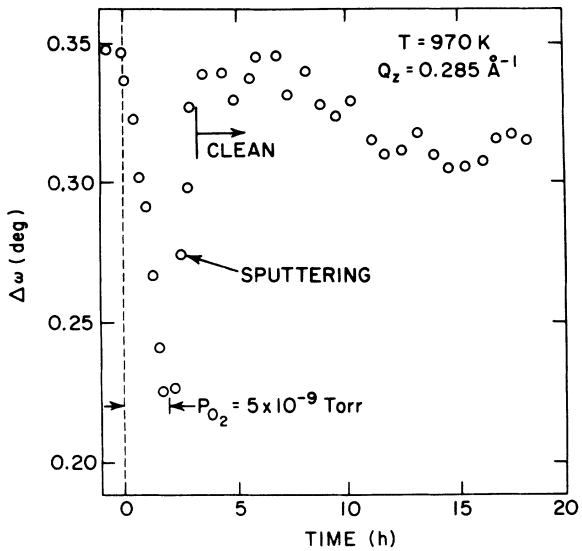

FIG. 5. The effect of O_2 for sample 2 at 970 K. A pressure of 5×10^{-9} Torr of O_2 induces faceting which reduces the peak width $\Delta\omega$. Sputtering restores the surface to a clean state. Note that under the clean conditions the sample would take several days to reach the faceted state.

ple 2) at $\phi=90°$. A clean surface was prepared at $t=0$ h. Then, an ambient pressure of 5×10^{-9} Torr of O_2 was introduced into the chamber and the line shape monitored as a function of time. Immediately after the introduction of the oxygen the linewidth started decreasing, as would also have occurred had the temperature been lowered. Here,the temperature was fixed at $T=970$ K. As soon as the O_2 was pumped out and the surface cleaned by Ar^+-ion bombardment the linewidth returned to its original value and very slowly decreases thereafter.

VI. DISCUSSION

It is worth discussing what behavior would be expected for the Fresnel reflectivity if at low temperatures the ECS of copper exhibits a slope discontinuity where the (110) facet meets other orientations, while at high temperatures it does not. In general, the magnitude of the slope discontinuity can depend on the azimuth about (110) and upon the temperature. The existence of a slope discontinuity implies that there is a range of orientations of the surface that do not exist in thermal equilibrium. Thus a slope discontinuity is directly related to a hill-and-valley structure. By cutting a crystal at some orientation with respect to the crsytalline axes, a particular boundary condition is imposed upon the surface. If the misalignment of the crystal falls outside of the disallowed range, the surface will conform to that misorientation. If the misalignment lies within the disallowed range, a hill-and-valley structure results. The gross features of our data can be understood on this basis. Further work, with better Cu surfaces, will resolve the remaining questions. (i) What are the coexisting phases at low temperatures? (ii) What is the nature of the fluctuations at high temperatures? (iii) How does the phase behavior depend on the orientation of the misalignment?

ACKNOWLEDGMENTS

We are particularly grateful to B. Larson, J. Budai, and D. Zehner of Oak Ridge National Laboratory for providing the copper crystals and to Peter Tackas of the Brookhaven National Laboratory for optical studies of these crystals. We would like to thank J. Axe, D. Fisher, D. Gibbs, G. Held, P. Horn, D. Huse, M. Wortis, and D. Zehner for useful discussions. S.G.J.M. acknowledges hospitality of the Brookhaven National Laboratory Physics Department during the course of this work. This work was supported by the Division of Materials Research, U.S. Department of Energy, under Contract No. DE-AC02-76CH00016.

*Present address: Department of Physics, Massachusetts Institute of Technology, Cambridge, MA 02139.

[1]C. Herring, Phys. Rev. **82**, 87 (1951).
[2]C. Rottman and M. Wortis, Phys. Rev. B **29**, 328 (1984).
[3]R. J. Phaneuf and E. D. Williams, Phys. Rev. Lett. **58**, 2563 (1987).
[4]G. Binnig and H. Rohrer, Surf. Sci. **152/153**, 18 (1985).
[5]A. Braslau, P. S. Pershan, G. Swislow, B. M. Ocko, and J. Als-Nielsen, Phys. Rev. A **38**, 2457 (1988).
[6]B. M. Ocko, A. Braslau, P. S. Pershan, J. Als-Nielsen, and M. Deutsch, Phys. Rev. Lett. **57**, 94 (1986).
[7]S. G. J. Mochrie, Phys. Rev. Lett. **59**, 304 (1987).
[8]S. Dietrich and H. Wagner, Z. Phys. B **56**, 207 (1984).
[9]S. K. Sinha, E. B. Sirota, S. Garoff, and H. B. Stanley, Phys. Rev. B **38**, 2297 (1988).
[10]D. A. Bruce, J. Phys. Chem. C **14**, 5195 (1981).
[11]S. R. Andrews and R. A. Cowley, J. Phys. C **18**, 6427 (1985).
[12]A. M. Afanas'ev, P. A. Aleksandrov, S. S. Fanchenko, V. A. Chaplanov, and S. S. Yakimov, Acta Crystallogr. Sect. A **42**, 116 (1986).
[13]J. Rowlinson and B. Widom, in *Molecular Theory of Capillary* (Oxford University Press, New York, 1983).
[14]M. P. A. Fisher, D. S. Fisher, and J. D. Weeks, Phys. Rev. Lett. **48**, 368 (1982).
[15]D. S. Fisher and J. D. Weeks, Phys. Rev. Lett. **50**, 1077 (1983).
[16]B. Gavish and V. Imry, J. Chem, Phys. **65**, 139 (1976).
[17]L. D. Gibbs, B. M. Ocko, D. M. Zehner, and S. G. J. Mochrie, Phys. Rev. B **38**, 7303 (1988), this issue.
[18]K. D. Stock and E. Menzel, Surf. Sci. **61**, 272 (1976).
[19]G. A. Held, J. L. Jordan-Sweet, P. M. Horn, A. Mak, and R. J. Birgeneau, Phys. Rev. Lett. **59**, 2075 (1987).
[20]K. S. Liang, E. B. Sirota, K. L. D'Amico, G. J. Hughes, and S. K. Sinha, Phys. Rev. Lett. **59**, 2447 (1987).
[21]J. Lapujoulade, J. Perreaud, and A. Kara, Surf. Sci. **129**, 59

(1983).
[22]M. den Nijs, E. K. Riedel, E. H. Conrad, and T. Engel, Phys. Rev. Lett. **55**, 1689 (1985).
[23]Graciously provided by D. M. Zehner.
[24]M. Wortis (private communication).
[25]G. Ertl, Surf. Sci. **6**, 208 (1967).
[26]F. H. P. M. Habraken and G. A. Bootsman, Surf. Sci. **87**, 333 (1979).
[27]C. S. Lent and P. I. Cohen, Surf. Sci. **139**, 121 (1984).

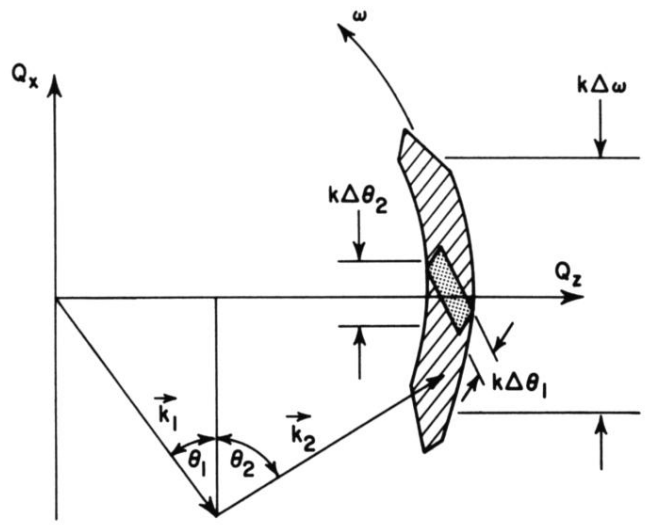

FIG. 1. The x-ray resolution volume projected onto the scattering plane. The shaded area is the resolution trapezoid defined by the spread of the incoming beam ($\Delta\theta_1$) and the acceptance of the detector slit ($\Delta\theta_2$). The resolution area swept out by scanning ω over a range $\Delta\omega$ is given by the hatched arc.